

# GIS-Based Frequency Ratio Model for Mapping the Potential Zoning of Groundwater in the Western Desert of Iraq

Prof. Dr. Mudhaffar S.Hasan AL-Zuhairy, Assis. Prof. Dr. Alauldeen Abdulrahman Hasan, Fadhil Mezher Shnewer

**Abstract**— Combination of remote sensing (RS) data with the geographical information system (GIS) for the investigation of groundwater (GW) resources has become an advance in the field of GW researches, which helps in evaluating, protecting and monitoring GW resources. The aim of this paper is to apply a bivariate statistical model such as frequency ratio (FR) for mapping of GW potential at the region of interest as a part from Iraqi western desert (located at Al-Ramadi and Shithatha). The exploration of GW in this area is a very important step to increase and develop the water resources because the absence of surface water in that region.

The FR method has not been applied to delineate GW potential in Iraq so far, and this contribution is uniqueness of this paper. Furthermore, this study contains the analysis of the spatial associations between GW wells data and numerous GW conditioning elements such as slope, altitude, stream density, aspect, fault, curvature, lithology, stream power index (SPI), soil, topographic wetness index (TWI), Normalized Difference Vegetation Index (NDVI) and rainfall for this region. Those elements are affecting the occurrences of GW, and were derived from satellite imagery, relevant government institutions and geological data. The thematic map for each element was prepared using GIS software. The GW wells (43 wells) used in this study were obtained from ministry of water resources - general authority for groundwater in Iraq. All observed GW wells were randomly separated into two groups: 30 wells as a training data assigned to the analysis with model (70 % of the total wells), and 13 wells as a testing data allocated for model's results validation (remaining 30 %). All element layers were combined and modelled using the suggested approach to generate the map of GW potential areas. The final GW map included five potential classes namely "very high", "high", "moderate", "low" and "very low" susceptible zones. The model's outcomes acquired in this research were validated with the GW wells data using Area Under the Curve (AUC) method. The validation of the results showed that the values of AUC were 57%, 53%, of success and prediction rate respectively. The outcomes attained from the present study indicated that the statistical model can offer an influential tool for delineation of GW resource. One of recommendations of this study is to apply the same proposed model in exploration of GW in other areas with the same conditioning parameters, but with higher accuracy to obtain higher precision results and compare them with the current study.

**Index Terms**— Groundwater potential, GW, Frequency ratio, Geographic information systems, GIS, Remote sensing, RS.

## 1 INTRODUCTION

Groundwater (GW) is one of the most important source of water that offers to the requirements in all climatic areas in the world and is the most valuable and dependable source of water [1]. It is formed by snowmelt water or rain-water that leaks down through the soil and into the fundamental rocks [2]. GW has several advantages compared with the surface water; it is more preserved from the contagions and pollutants, is less visible to permanent and seasonal fluctuations, is much regularly extent over large regions and has a superior quality. GW meets the need in the nonexistence of surface water. GW facilities do not require large investments where they can be gradually advanced [3].

Iraqi lands have suffered more than two decades of water shortages to fulfil future requirements due to lack of rain-fall and because of the absence of best employment of water resource by making more advanced irrigation system.

Other reasons regard to external affairs is that Syria, Turkey and Iran have built a lot of dams in the upstream of rivers which flow through Iraq. For instance, GAP project (Güneydogu Anadolu Projesi) which is the South-eastern Anatolia Project - Turkey by building 22 dams on Euphrates and Tigris River [4]. When the completion of GAP project, it leaves a negative influence on the surrounding area, for example Syria will lose about 40% of the share of the Euphrates and Iraq will lose approximately 90% causing an upsurge in pollution and desertification problems. In Iraq, the need for water for agriculture purpose is about 65% and for domestic consumptions are estimated 80% of both rivers [5].

The study area is one of the regions that will be greatly affected by the conditions revealed above because it will stop any future plans for the development of irrigation systems through the use of Euphrates water. The area under study lacks to surface water, except for some floods, which seldom happen during the rainy season. Since GW is the only available source for water in the research area, there must be serious and detailed studies on this subject. The rising demand of GW suggests new methods which can enhance conventional methods for GW potential valuation using data removal and sta-

• Fadhil Mezher Shnewer is currently pursuing masters degree program in surveying engineering in Engineering Technical College-Baghdad, Iraq, PH- 009647705500960. E-mail: Fadhilmezher@yahoo.com

tistical approach for present practice. The traditional techniques compared to new approach were typically relying on expert estimation and local information. The current study focuses on the study of GW in an important part of Iraq using GIS-modeling to predict the occurrence of GW potential. The traditional methods for exploration of GW such as geophysical, hydrological and geological approaches required economic investments with high costs in comparison to RS and GIS approach [6]. The data derived from satellite can offer rapid and suitable baseline information about the conditioning parameters affected the groundwater occurrence and movement [7]. The application of RS and GIS systems has successfully proved the combination of several thematic maps (TM) of terrain in numerous studies which has appeared as a necessary tool in the identification of GW sites.

Several studies have been conducted for mapping of GW potential using GIS-based models and RS data. Musa et al. (2000) [8], studied the GW potential zones in Malaysia. They used the integration of remote sensing with GIS technique. The final map was gained through the combination of all thematic layers using DRASTIC model. They concluded that GIS-based model is an appropriate technique for GW potential zoning in the rocky regions. Oh et al. (2011) [9], applied GIS-based Frequency Ratio approach and sensitivity analysis to evaluate the associations between GW specific capacity (SPC) and its related hydrological influences to measure the sensitivity of each factor and to delineate GW potential mapping in Korea. Ozdemir (2011) [10], applied three approaches, logistic regression, weights of evidence and frequency ratio, in order to mapping of GW spring potential in Turkey. This study was based on the association between GW spring positions which were identified from a topographic map, and their relevant influences. This study demonstrated that the WOE and FR models are comparatively well estimators. Magesh et al. (2011) [11], applied RS techniques with GIS to delineate the zones of GW availability in India. They used MIF technique (multi-influencing-factor) to calculate the score and weight for each element's classes. The final groundwater potential map was estimated based on the combination of these weighted values through GIS system. Manap et al. (2012) [12], applied GIS-based FR model to delineate the maps of groundwater potential in Malaysia depending on the spatial relation between groundwater yield and the conditioning elements. This is the first study in which the FR model was applied in groundwater potential in Malaysia. Manap et al. (2013) [13], used knowledge driven model (weighted linear combination model) - based GIS in order to GW potential mapping in Malaysia. This type of model depends on expert opinion in the guessing process. Nampak et al. (2014) [3], applied GIS-based Evidential Belief Function (EBF) approach in order to mapping of GW potential zones in Malaysia. Then, the Logistic Regression (LR) model was applied in order to compare the final outcomes between the two models. Zeinolabedini and Esmaeily (2015) [14], used GIS-based AHP model (Analytic Hierarchy Process) to identify GW potential in Iran. The weighted values for all parameters used were obtained using this model, and the final map was generated based on these weights.

The FR model is one of the types of data driven tech-

niques which based on real data to estimate the event. These types of models have not been applied to delineate groundwater potential in Iraq so far. In this study, the FR model was applied for mapping the potential zoning for the region located at Al-Ramadi and Shithatha as a part of Iraqi western desert. The associations among groundwater wells and GW conditioning factors containing rainfall, soil, elevations, lithology, curvature, TWI, aspect, faults, slope, SPI, NDVI and drainage density was also studied. The result of this paper may be useful for the competent authorities in the field of groundwater in Iraq for GW exploration and evaluation.

## 2. STUDY AREA

The study area is part from Iraqi western desert and locates in two zones at Al-Ramadi and Shithatha. It lies between 42° 02' 12" E to 42° 59' 06" E and 32° 43' 55" N to 33° 25' 45" N (Fig. 1) covering an area about 5391.65 km<sup>2</sup>. It includes numerous of large wadis like w. Ghadaf, w.Thmail and w. Mahammadiyah. The climate in the research area is dry and hot in general. It receives an average of 100-150 (mm) annual rainfall with a maximum temperature of 43°C and a minimum temperature of 16° C [15]. The majority of the study area is not inhabited where most people prefer to live near the Euphrates River and lakes. The study area is commonly classified as a flat zone, increasing in altitude westwards. The landscape of the study area is characterized by the plateaus that are dismembered by dense valleys; some of them extend for a few kilometers, while others extend to large kilometers. The landscape is also representative by one hill (Garat Al-Shutub), located in the southeast of the study area. The topographic incline of the study area increases from east to west. The lowest point near of Euphrates River which has an elevation 81m and the highest point located in the west with elevation 465 m.

## 3. DATA USED

As this paper aims to produce map showing the possibility of GW occurrence, it is necessary to create several parameters that are believed to affect the occurrence of GW and thus finding the spatial correlation between these parameters and GW wells which scattered in a given area. In this paper, twelve factors were selected to predict the existence of groundwater in the study area using FR model. The factors are rainfall, soil, altitudes, lithology, curvature, TWI, aspect, faults, slope, SPI, NDVI and drainage density. The topographic elements (altitude, slope, aspect and curvature) were derived from Digital Elevation Model (DEM). The DEM of the study area has a spatial resolution of 30 m and it has the best available accuracy for free in Iraq at the moment. Also, several water-related elements such as TWI, drainage density and SPI were gotten from the DEM. The geological map of 1:250,000 scale was provided from University of Technology - Geomatic branch as a raster map and was digitalized in GIS to obtain the geological layers and faults. The soil map of 1:1000,000 scale as a raster map was obtained from Ministry of agriculture in Iraq then digitized to gain the soil layers. Rainfall data of past 31 years (1982-2013) was prepared from Iraqi Meteorological Organization and Seismology in excel file then the rainfall map was equipped by interpolation of data using Inverse Dis-

tance Weighted (IDW) method through GIS. The NDVI map of the study area was obtained from remote sensing imagery (Landsat 8 ETM+). Equation (1) used to compute the values of NDVI.

$$NDVI = (NIR - VIS) / (NIR + VIS) \quad (1)$$

Where: VIS and NIR: Represent the spectral reflectance measurements attained in the visible (red) and near-infrared regions, respectively.

The thematic map for each element was prepared through GIS (Fig.2 a-l). In this paper, the date of ground water such as number of wells, coordinates, depth and yield of wells were gained from ministry of water resources - general authority of groundwater in Iraq. The real pumping test of GW well e.g. m<sup>3</sup>/day is used to derive the yield of GW. The numbers of GW borehole wells in the study area are 43 wells. These wells were nominated for GW productivity analysis and randomly distributed into two sets (training (70%) and testing (30%)) [16]. A training dataset (30 groundwater wells) will be used in the analysis of statistical model, and testing dataset (13 groundwater wells) will be assigned for model validation (Fig.3).

#### 4. METHODOLOGY

In order to mapping of groundwater probability, there are four steps need to this purpose [10]: (1) Collection of data and building of spatial database for the GW linked conditioning aspects,(2)Valuation of GW probability through the connotations between the conditioning aspects and wells,(3) Check the results,(4) Then the results obtained should be described and interpreted. (Fig. 4) shows the general methodology that used in this paper.

**Frequency Ratio (FR) model** can be defined as the rrence of probability of a specified feature [17]. FR approach is statistical model (bivariate model) that has an application as simple tools for geospatial valuation and computation of the probabilistic association between dependent variable (the groundwater in this work) and independent variables (the factors that affect the occurrence of groundwater). It is ordinarily supposed that the existence of GW is estimated by GW conditioning elements, and future GW wells will happen under the same situations as past occurrences of GW. Keeping these suppositions in mind, a distinguishing line can be drawn between the correlation among GW well happening in an area and the GW conditioning influences and the correlation between GW wells not happening in an area and the GW conditioning influences. This method is proficient in viewing the connection between the factors that indicate the occurrence of GW and the wells of GW [9]. FR approach is greatly tood and easy to apply compared with other statistical proaches, particularly in operations that include inputs, computations and outputs. This model is considered as a well method in assessment the results of GW spring potential [10]. It

has been applied in multi-studies for example, mapping of GW potential, forest fire study and the vulnerability of landslide.

To apply the FR model, each conditioning element was changed to a raster grid with 30×30 m cells. The full number of cells in study area is 5990719 (total number of rows and columns is 2635 and 3024 respectively). The numbers of groundwater wells assigned to the analysis are 30 wells. The association detected between the location of groundwater wells and all the influences related groundwater forms the foundation of the analysis in this approach (only quantitative outcomes are achieved through this method). Equation (2) used to calculate the frequency ratio values.

$$FR = (A/B) / (C/D) = E/F \quad (2)$$

Where:

A: is the area of a class for each GW conditioning influence, B: is the total area of the each element, C: is the number of GW occurrences within the class area of the factor, D: is the number of total GW occurrences in the study area, E: is the percentage for area with regard to a class for the factor, F: is the percentage for the entire domain, FR: is the ratio of the area where groundwater occurred to the total area.

If the FR value is lower than 1 that indicates to lower relation and a value greater than 1 refer to higher connection [18].

#### 5. RESULTS AND DISCUSSION

For appreciation of GW potential areas using FR are based on the spatial relation between the scattering of observed GW wells and each conditioning element. Each conditioning influence is classified into different categories and each category has FR value. This value was estimated by taken into account each category of all the GW controlling element pixels affected by GW (%) and entire pixels (%). Quantile method [19] was chosen for classification with this model. Table (1) shows FR values for each range or element's kind. The lower value represents low potential of GW occurrence and the larger value denotes the high potential.

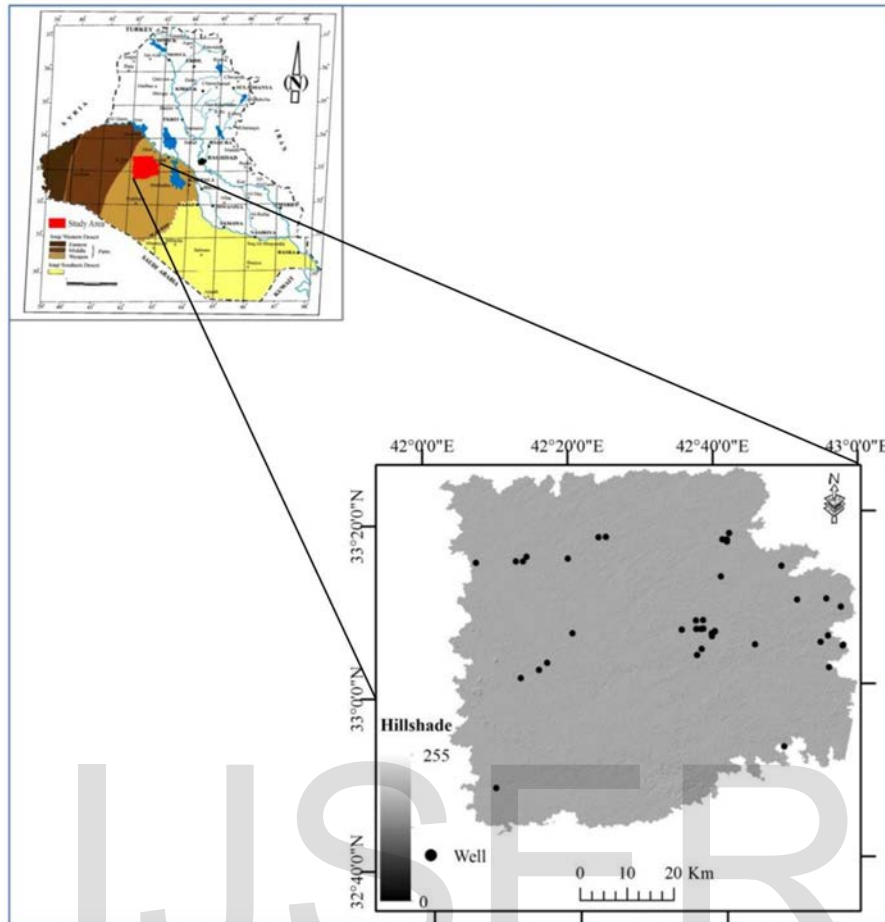
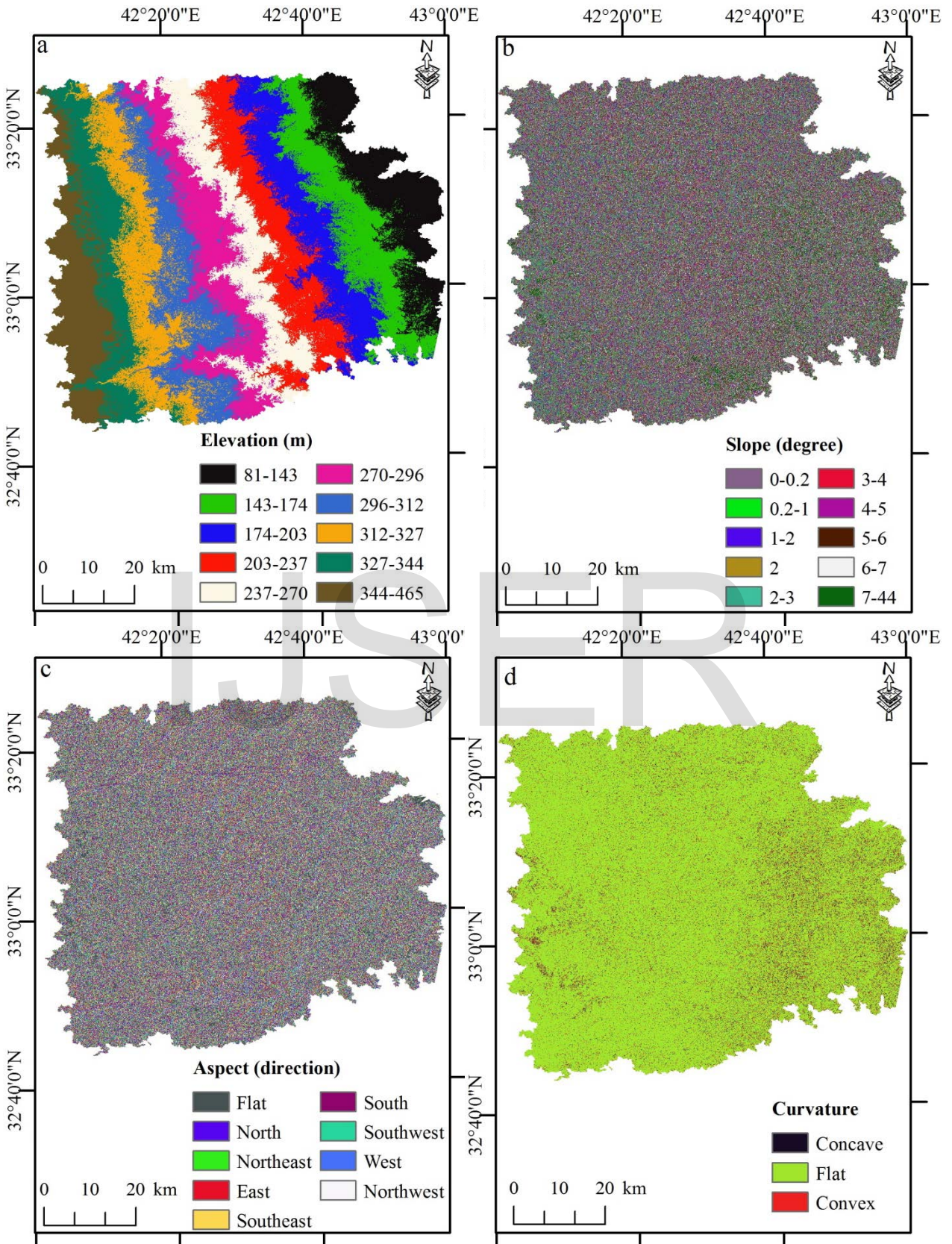
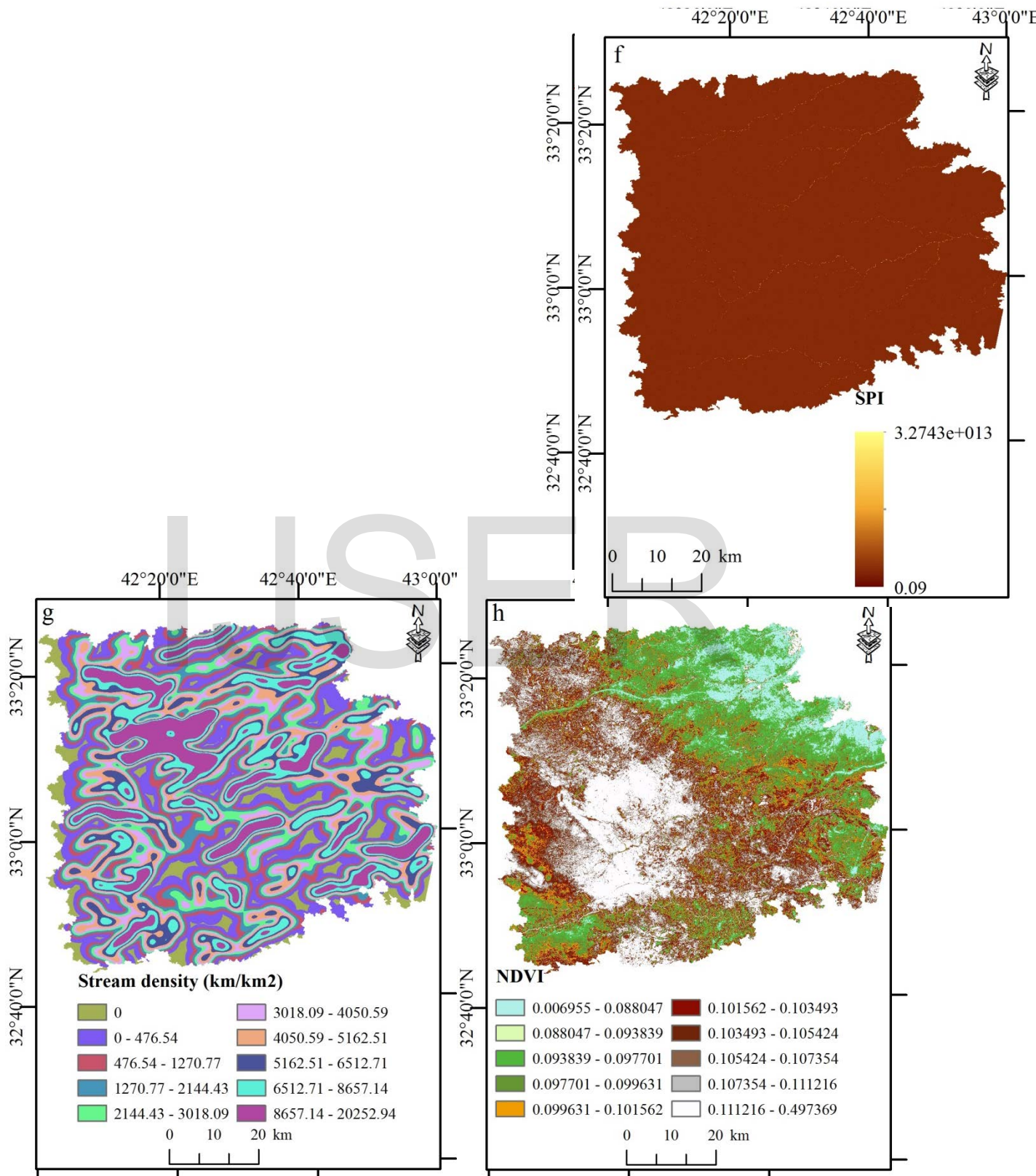


Fig.1. Location map of the study area.





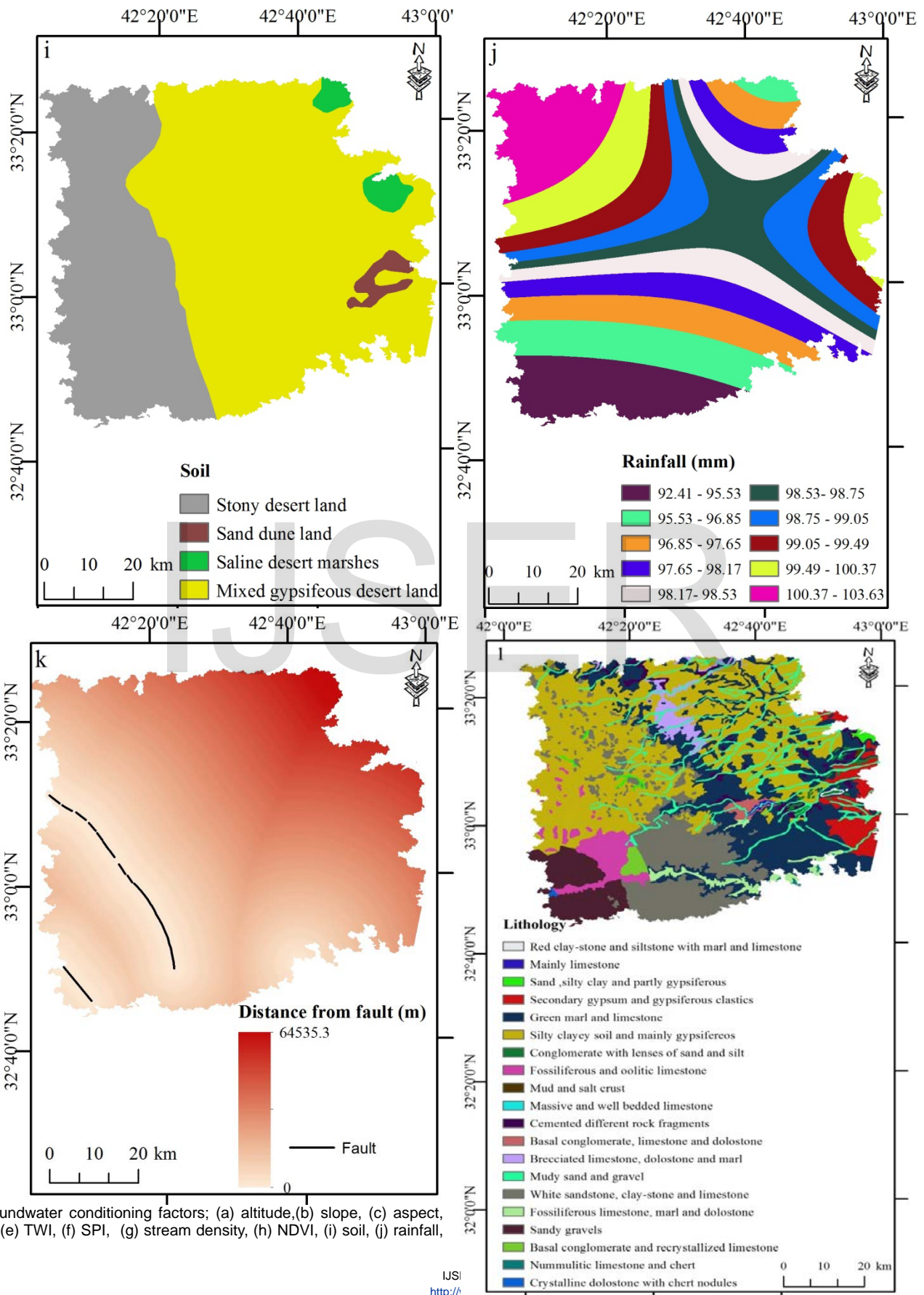


Fig.2. Groundwater conditioning factors; (a) altitude,(b) slope, (c) aspect, curvature, (e) TWI, (f) SPI, (g) stream density, (h) NDVI, (i) soil, (j) rainfall,

(d)  
(k)

fault, and (l) lithology.

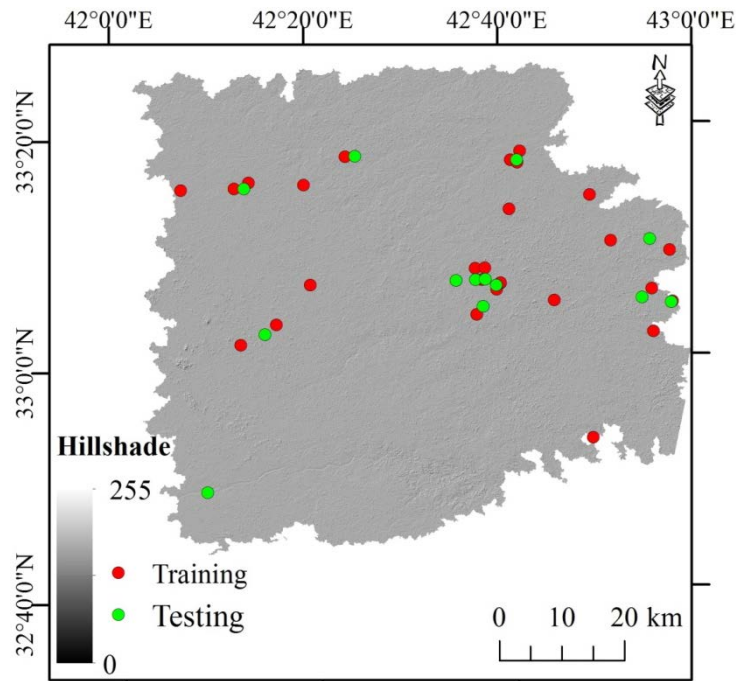


Fig.3. Groundwater wells locations in the study area

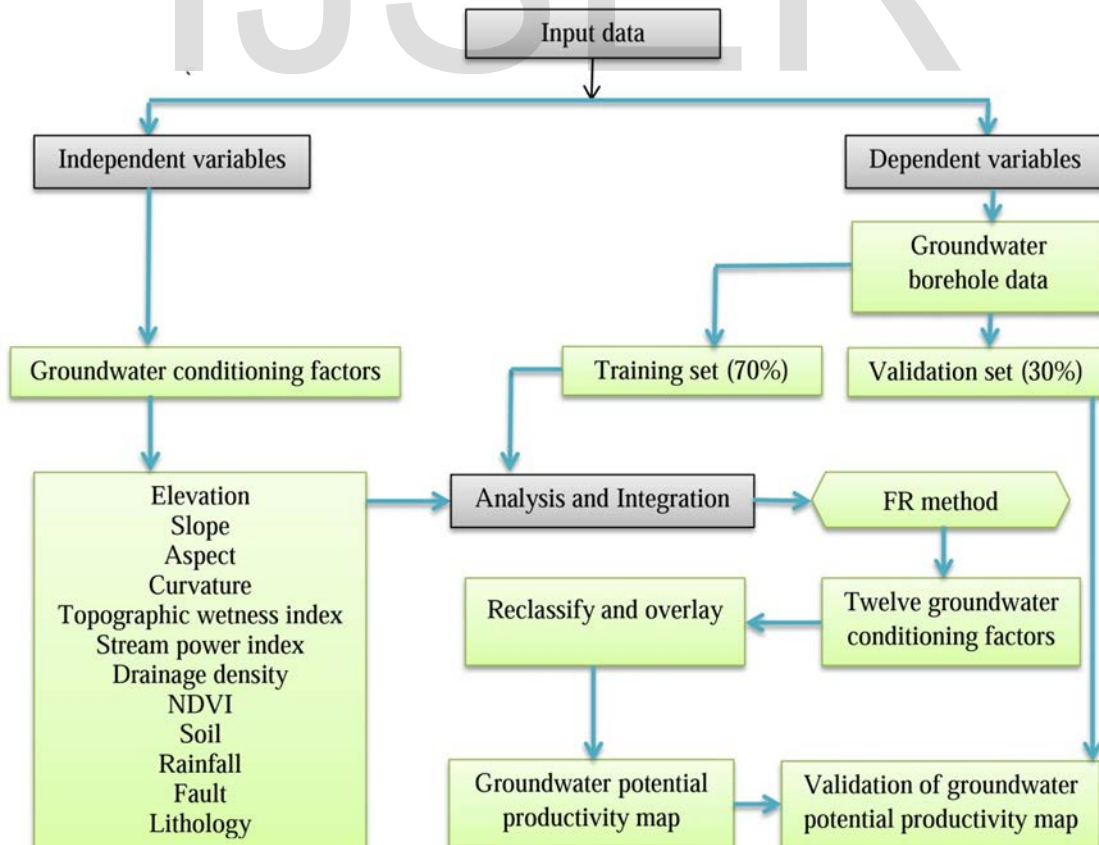




Fig.4. Overall methodology used in this paper

**TABLE 1**  
**FREQUENCY RATIO VALUE FOR CLASSES OF GROUNDWATER CONDITIONING FACTORS**

Factor	Range	No. of class pixel	(%) of class pixel(a)	Pixels in domain	% of Pixels in domain(b)	Frequenc Rtio ((b/a)*100)
<b>Elevation (m)</b>	81 - 143	612576	10.2	58	23.7	232
	143 - 174	618940	10.3	35	14.3	138
	174 - 203	600017	10.1	45	18.4	182
	203 - 237	603743	10	35	14.3	143
	237 - 270	596476	10	9	3.6	36
	270 - 296	605201	10.1	0	0	0
	296 - 312	622480	10.4	9	3.6	34
	312 - 327	615701	10.3	35	14.3	138
	327 - 344	563942	9.4	11	4.5	47
	344 - 465	551643	9.2	8	3.3	35
<b>Slope(degree)</b>	0 - 0.2	520123	8.7	10	4.1	47
	0.2 - 1	769523	12.8	46	18.8	146
	1 - 2	770570	12.9	34	13.9	107
	2	503433	8.4	23	9.4	111
	2 - 3	627551	10.5	35	14.3	136
	3 - 4	606524	10.1	10	10.2	100
	4 - 5	620278	10.4	25	6.1	58
	5 - 6	533879	8.9	15	6.9	77
	6 - 7	537160	8.9	17	10.2	114
	7 - 44	501678	8.4	25	6.1	73
<b>Aspect (direction)</b>	Flat	633574	10.6	16	6.5	61
	North	638755	10.7	33	13.5	126
	Northeast	731546	12.2	33	13.5	110
	East	682682	11.4	23	9.4	82
	Southeast	721179	12	31	12.7	105
	South	722636	12	34	13.9	115
	Southwest	638544	10.7	24	9.8	91
	West	575574	9.6	17	6.9	72
	Northwest	646229	10.8	34	13.8	128
<b>Curvature</b>	Concave	318921	5.3	15	6.1	115
	Flat	5289777	88.3	219	89.4	101
	Convex	382021	6.4	11	4.5	70
<b>TWI</b>	2.28 - 4.5	451798	7.6	14	5.7	75
	4.5- 5.06	757168	12.6	25	10.2	80
	5.06 - 5.62	711250	11.9	27	11	92
	5.62 - 7.56	705032	11.8	41	16.7	142
	7.56 - 12	507764	8.5	19	7.8	91
	12 - 13.12	560017	9.3	26	10.6	113
	13.12 - 14.51	589966	9.8	26	10.6	107
	14.51 - 16.17	579851	9.7	24	9.8	101
	16.17 - 21.73	582979	9.7	35	14.3	146
	21.73 - 37.71	544894	9.1	8	3.3	35

<b>SPI</b>	0 - 0.09	25805	0.4	0	0	0
	0.09 - 128403920984.4	5946559	99.3	245	100	100
	128403920984.4 - 256807841968.8	6574	0.12	0	0	0

Table 1 (Continued)

Factor	Range	No. of class pixel	(%) of class pixel(a)	Pixels in domain	% of Pixels in domain(b)	Frequency ratio ((b/a)*100)
	256807841968.8 - 385211762953.1	2836	0.05	0	0	0
	385211762953.1 - 642019604921.8	2676	0.04	0	0	0
	642019604921.8 - 1027231367874.8	1864	0.03	0	0	0
	1027231367874.8 - 1540847051812.2	1276	0.02	0	0	0
	1540847051812.2 - 2439674498702.6	1116	0.02	0	0	0
	2439674498702.6 - 4237329392483.5	1016	0.02	0	0	0
	4237329392483.5 - 2614595930023.6	997	0.02	0	0	0
<b>Stream density</b>	0	336200	5.6	9	3.7	65
	0 - 476.54	961978	16.1	9	3.7	22
	476.54 - 1270.77	628723	10.5	42	17.1	163
	1270.77 - 2144.43	589546	9.9	2	0.8	8
	2144.43 - 3018.09	577318	9.6	40	16.3	169
	3018.09 - 4050.59	613777	10.2	27	11	107
	4050.59 - 5162.51	580057	9.7	20	8.2	84
	5162.51 - 6512.71	571878	9.5	52	21.2	222
	6512.71 - 8657.14	577614	9.7	26	10.6	110
	8657.14 - 20252.94	553628	9.2	18	7.4	79
<b>NDVI</b>	0.006955 - 0.088047	410375	6.9	31	12.7	184
	0.088047 - 0.093839	808968	13.5	51	20.8	154
	0.093839 - 0.097701	872672	14.6	47	19.2	131
	0.097701 - 0.099631	522783	8.7	22	9	102
	0.099631 - 0.101562	575961	9.6	28	11.4	118
	0.101562 - 0.103493	612723	10.2	24	9.8	95
	0.103493 - 0.105424	597311	10	17	7	69
	0.105424 - 0.107354	507933	8.5	4	1.6	19
	0.107354 - 0.111216	641873	10.7	4	1.6	15
	0.111216 - 0.497369	440120	7.3	17	6.9	94
<b>Distance from fault</b>	0 - 3796.19	585896	9.8	18	7.3	75
	3796.19 - 7339.31	629286	10.5	0	0	0
	7339.31 - 10376.26	626130	10.4	8	3.3	31
	10376.26 - 13919.38	603145	10.1	18	7.3	73
	13919.38 - 18980.97	616263	10.3	18	7.3	71
	18980.97 - 24042.56	604771	10.1	9	3.7	36
	24042.56 - 29357.23	581782	9.7	27	11	113
	29357.23 - 35937.30	598723	10	71	29	290
	35937.30 - 44035.85	570816	9.5	34	13.9	145
	44035.85 - 64535.30	576479	9.6	42	17.2	178
<b>Lithology</b>	Red clay-stone and siltstone with marl and limestone	5426	0.09	0	0	0
	Mainly limestone	7250	0.12	0	0	0
	Sand ,silty clay and partly gypsiferous	28634	0.48	9	3.7	768
	Secondary gypsum and gypsiferous clastics	208177	3.47	23	9.4	270
	Green marl and limestone	1254501	20.94	40	16.3	77

Silty clayey soil and mainly gypsiferous	2175056	36.31	129	52.6	145
Conglomerate with lenses of sand and silt	35777	0.6	0	0	0

Table 1 (Continued)

Factor	Range	No. of class pixel	(%) of class pixel(a)	Pixels in domain	% of Pixels in domain(b)	Frequency ratio ((b/a)*100)
	Fossiliferous and oolitic limestone	216599	3.62	0	0	0
	Mud and salt crust	3164	0.05	0	0	0
	Massive and well bedded limestone	1018	0.02	0	0	0
	Cemented different rock fragments	106733	1.77	5	2	114
	Basal conglomerate, limestone and dolostone	34474	0.58	0	0	0
	Brecciated limestone, dolostone and marl	123830	2.07	0	0	0
	Mudy sand and gravel	435341	7.26	31	12.7	174
	White sandstone, clay-stone and limestone	880591	14.7	0	0	0
	Fossiliferous limestone, marl and dolostone	91128	1.52	8	3.3	214
	Sandy gravels	335520	5.6	0	0	0
	Basal conglomerate and recrystallized limestone	39265	0.66	0	0	0
	Nummulitic limestone and chert	4692	0.08	0	0	0
	Crystalline dolostone with chert nodules	3543	0.06	0	0	0
<b>Soil</b>	Stony desert land	2007303	33.5	45	18.4	54
	Sand dune land	92176	1.5	9	3.7	238
	Saline desert marshes	124069	2.1	8	3.3	157
	Mixed gypsiferous desert land	3769743	62.9	183	74.6	118
<b>Rainfall</b>	92.406418 - 95.532164	587792	9.8	0	0	0
	95.532164 - 96.852902	605028	10.1	0	0	0
	96.852902 - 97.645345	602767	10.1	0	0	0
	97.645345 - 98.17364	595939	9.9	34	13.9	139
	98.17364 - 98.525837	602180	10.1	35	14.3	142
	98.525837 - 98.74596	648324	10.8	70	28.6	264
	98.74596 - 99.054132	634288	10.6	18	7.3	69
	99.054132 - 99.494378	589991	9.9	17	6.9	70
	99.494378 - 100.37487	576611	9.6	44	18	186
	100.37487 - 103.63269	547799	9.1	27	11	120

The probability of GW occurrence is usually diminutions with the value of altitude. High slope angle leads to surface run-off increase, and hence the infiltration process will be decreased [20]. If the slope was bigger than 35 degrees the probability of GW potential is decreased because it limits the favorability of GW [21]. A high slope generates high TWI. There is a good connection between TWI and the occurrence of GW, where the increases of TWI value will result higher potential of GW. However, there is a bad relation between GW productivity and SPI [3]. The denser of NDVI indicates low probability of GW occurrence, and the GW frequency increased when the distance from fault increased. According to the table (1), the probability of GW occurrence is low in the zones which have high elevation, high slope and convex curvature. Also,

the correlation between GW probability with TWI, SPI and stream density is positive. In the case of NDVI, there is a low correlation between the denser of NDVI and GW probability. The regions distant from fault have high GW probability and vice versa. Concerning lithology, Sand, silty clay and partly gypsiferous records the highest value of GW probability. Sand dune land is the soil type which has high correlation with GW probability. Only the class (98.525837 - 98.74596) which shows a high correlation with respect to the rainfall.

After calculating FR values for each element depending on the association among conditioning elements and GW productivity, these values will be integrated (using raster calculator in GIS) to obtain the map of GW potential index. The following equation was used to derive this map.

$$GWPI = Fr_1 + Fr_2 + Fr_3 + Fr_4 + \dots + Fr_n \quad (3)$$

Where: GWPI: the groundwater occurrence potential index, FR: the frequency ratio of a factor, n: the total number of input factors.

The map of GW potential was quantitatively established using potential index value of GW where the minimum value was 410 and the maximum was 2455 (Fig. 5).

In the final step, the GWPI map was classified into five potential zones to assist on the interpretation of GW potential map. Rating process does not rely on any statistical base from which to automatically classify as not having to this rule so far [19]. Therefore, most of the researchers resorted to expert opinion in the rating process. Consequently, five ground water susceptibility classes were determined using Quantile method for classification [18] as follow: very low (40%), low (20%), moderate (20%), high (10%) and very high (10%) (Fig. 6). This study shows that the larger part of the study area (40.7% of the whole area) represent very low GW potential. The parts with low GW form about 20.7%, while moderate potential forms about 19.8%. Each one of the high and very high potential forms 9.4%.

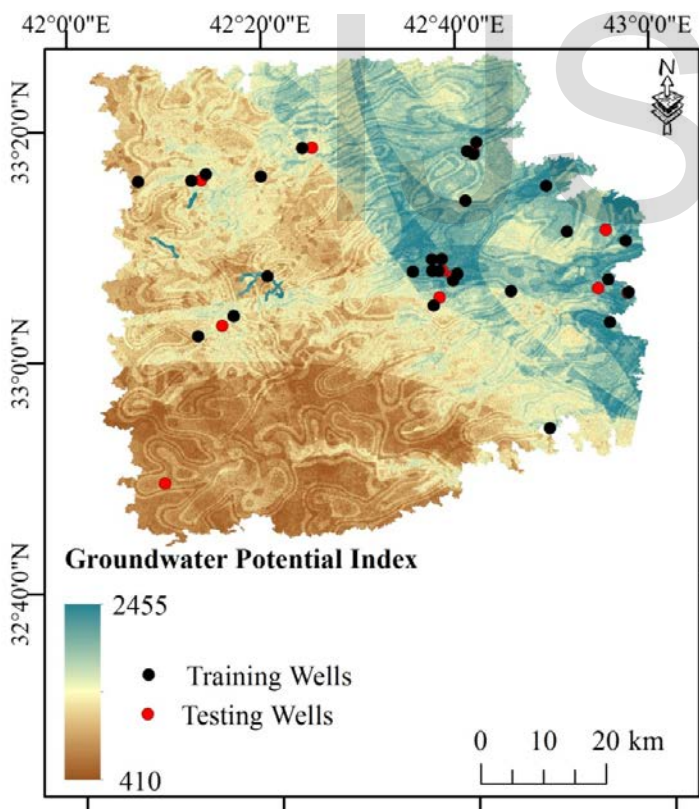


Fig.5. Groundwater potential index using frequency ratio approach

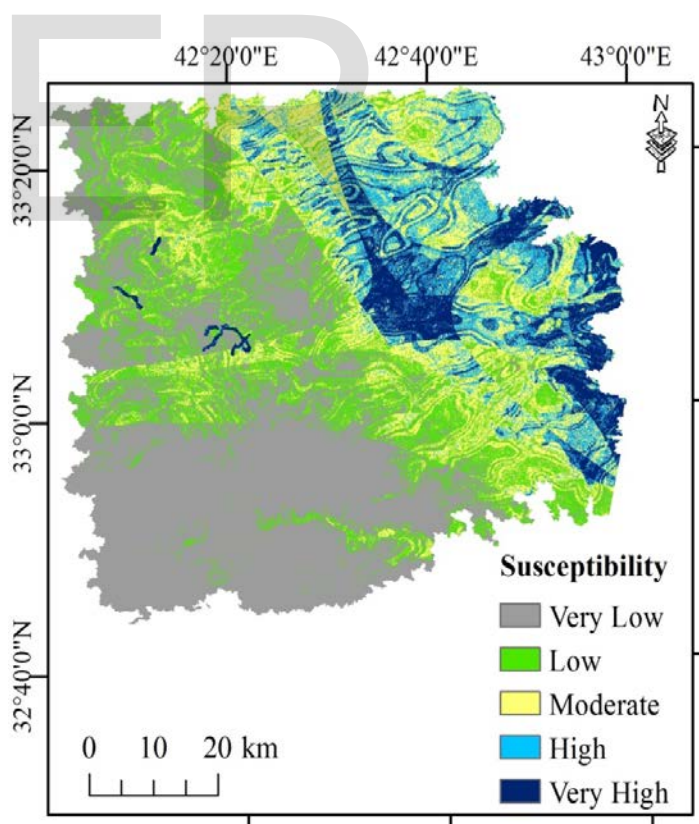


Fig.6. Groundwater potential zone using FR approach

## 6. VALIDATION OF THE GROUNDWATER POTENTIAL MAP

After obtaining the GW potential map through the application of FR model, the results must be validated. The validation of model is an important step to evaluate the outcomes where the model without validation has no scientific meaning [22]. The results were verified by comparing the outcomes obtained from this model with the location data of the existing GW wells in the area, and "the Area Under the Curve" (AUC) method [7] was used for validation. AUC is one of the most significant methods used to evaluate the accuracy of predictive models in environmental specialties [23]. The prediction and success ratio of the model is calculated using this method. Valuation of success and prediction -rate is a necessary product for any scheme [24]. By overlapping the map of GW potential with the training GW wells locations, accumulative percentage of the GW occurrence (beginning from the maximum values to the minimum values of GWPI) were computed (Fig.7). Then, the curves of the success-rate were achieved through these cumulative percentages. The validation of the result showed that the value of the AUC were 0.57, which be equivalent to 57% of success accuracy for FR method. Since the method of success rate depends on the location of training GW wells which were used during the analysis in the model, thus the method is not considered a suitable to evaluate the prediction competence of the models [18]. Nevertheless, this method may aid to define how well the resultant GW potential map has categorized the zones of standing wells. The process of predicting the occurrence of GW in the area can be defined by the method of prediction rate which was conducted by the use of testing wells (i.e. 13 samples) that were not used in the analysis with the model [18]. As displayed in (Fig.7) the AUC values for the curve of prediction rate for GW potential map using FR method was 0.53, which be equivalent to 53% of prediction accuracy. This result indicates that the FR model is less accurate for groundwater potential zoning in the study area. This may be because the low accuracy of the data used or due to the nature and situations of the region of interest.

and develop the water resources in the Iraqi western desert. Because of the lack of surface water in the study area, using groundwater is a good solution to that problem to satisfy the agricultural, industrial and other important consumptions needed by human and hence increasing urban growth at that region in the future.

2- To map GW potential zones, the major step was the creation of a data base including GW controlling parameters which influence the GW occurrence. Those parameters were combined using the suggested model, which designated the association between GW yield data and the preparing parameters.

3- This study illustrated that the FR model is low accuracy for GW potential in study area. The validation process for this model showed that the prediction and success ratio are 53%, 57% respectively. While previous studies have proved the model efficiency in the prediction of groundwater.

4- This study indicates that the combination of RS data and GIS-based model can offer an influential tool for delineation of GW resources.

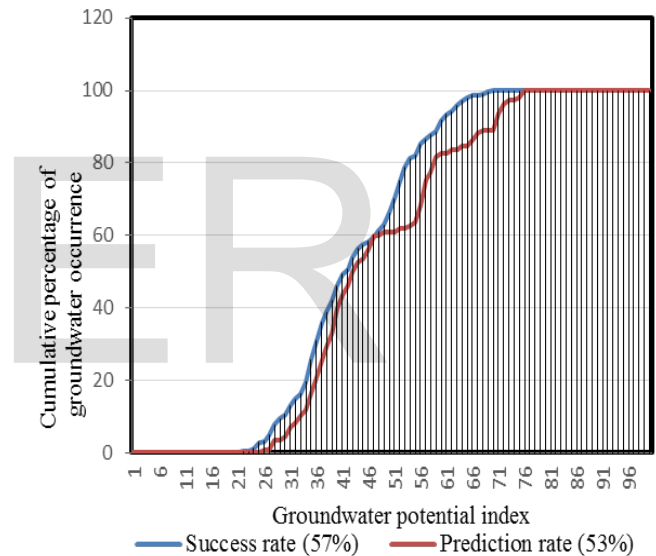


Fig.7. The success and prediction rate of FR model

## 7. CONCLUSIONS

1- The investigation of GW is an important step to increase

## REFERENCES

- [1] Todd, D. K. and Mays, L. W. (2005). *Groundwater Hydrology*. 3rd edition, John Wiley and Sons, NJ, pp. 636.
- [2] Banks, D., Robins, N. S., and Robins, N. (2002). *An introduction to groundwater in crystalline bedrock*. Norges Geologiske Undersokelse.
- [3] Nampak, H., Pradhan, B., and Manap, M. A. (2014). Application of GIS based data driven evidential belief function model to predict groundwater potential zonation. *Journal of Hydrology*, 513, 283-300.
- [4] Jongerden, Joost, Dams and Politics in Turkey: Utilizing Water Development Conflict, MiddelEast Policy, the Social Sciences Department of the Wageningen University in the Netherlands Vol.XVII, No. 1, Spring 2010.
- [5] Al-Muqdadi, S. W. (2012). *Groundwater investigation and modeling-western desert of Iraq*. Technische Universität Bergakademie Freiberg, PhD. Thesis.
- [6] Singh, A. K., and Prakash, S. R. (2003). An integrated approach of remote sensing, geophysics and GIS to evaluation of groundwater potentiality of Ojhala sub-watershed, Mirzapur district, U.P., India. <http://www.gisdevelopment.net>. Retrieved 25 August 2007.
- [7] Meijerink AMJ (2000) *Groundwater*. In: Schultz GA, Engman ET (eds) *Remote sensing in hydrology and water management*. Springer, Berlin, pp 305-325.
- [8] Musa, K. A., Akhir, J. M., and Abdullah, I. (2000). Groundwater prediction potential zone in Langat Basin using the integration of remote sensing and GIS. <http://www.gisdevelopment.net>. Retrieved 24 July 24, 200
- [9] Oh, H-J., Kim, Y-S., Choi, J-K., Park, E. and Lee, S. (2011). GIS mapping of regional probabilistic groundwater potential in the area of Pohang City, Korea. *Journal of Hydrology*, 399(3-4), 158-172. DOI:10.1016/j.jhydrol.2010.12.027.
- [10] Ozdemir, A. (2011) GIS-based groundwater spring potential mapping in the Sultan Mountains (Konya, Turkey) using frequency ratio, weights of evidence and logistic regression methods and their comparison. *Journal of Hydrology*, 411(3-4):290-308 DOI:10.1016/j.jhydrol.2011.10.010.
- [11] Magesh, N. S., Chandrasekar, N., & Soundranayagam, J. P. (2012). Delineation of groundwater potential zones in Theni district, Tamil Nadu, using remote sensing, GIS and MIF techniques. *Geoscience Frontiers*, 3(2), 189-196.
- [12] Manap, M. A., Nampak, H., Pradhan, B., Lee, S., Sulaiman, W. N. A., and Ramli, M. F. (2012). Application of probabilistic-based frequency ratio model in groundwater potential mapping using remote sensing data and GIS. *Arabian Journal of Geosciences*, 7(2), 711-724.
- [13] Manap, M.A., Sulaiman, W.N.A., Ramli, M.F., Pradhan, B., Surip, N. (2013). A knowledge-driven GIS modeling technique for groundwater potential mapping at the Upper Langat Basin, Malaysia. *Arabian Journal of Geosciences*, 6 (5), 1621- 1637. <http://dx.doi.org/10.1007/s12517-011-0469-2>.
- [14] Zeinolabedini, M., & Esmaily, A. (2015). GROUNDWATER POTENTIAL ASSESSMENT USING GEOGRAPHIC INFORMATION SYSTEMS AND AHP METHOD (CASE STUDY: BAFT CITY, Kerman, IRAN). *International Archives of the Photogrammetry, Remote Sensing & Spatial Information Sciences*, 40.
- [15] Iraqi Meteorological Organization and Seismology, [www.meteoseism.gov.iq/](http://www.meteoseism.gov.iq/).
- [16] Pradhan B, Lee S, Buchroithner MF (2010a) Remote sensing and GIS-based landslide susceptibility analysis and its cross-validation in three test areas using a frequency ratio model. *Photogramm Fernerkun* 1:17-32. doi:10.1127/1432-8364/2010/0037.
- [17] Bonham-Carter, G. (1994). *Geographic information systems for geoscientists: modelling with GIS* (No. 13). Elsevier.
- [18] Pradhan, B. and Lee, S. (2010) Landslide susceptibility assessment and factor effect analysis: back propagation artificial neural networks and their comparison with frequency ratio and bivariate logistic regression modelling. *Environmental Modelling & Software*, 25:747-759.
- [19] Ayalew, L., Yamagishi, H., Marui, H., and Kanno, T. (2005). Landslides in Sado Island of Japan: Part II. GIS-based susceptibility mapping with comparisons of results from two methods and verifications. *Engineering Geology*, 81(4), 432-445.
- [20] Jaiswal, R. K., Mukherjee, S., Krishnamurthy, J., and Saxena, R. (2003). Role of remote sensing and GIS techniques for generation of groundwater prospect zones towards rural development—an approach. *International Journal of Remote Sensing*, 24(5), 993-1008.
- [21] Madrucci, V., Taioli, F. and Cesar de Araujo, C. (2008). Groundwater favorability map using GIS multicriteria data analysis on crystalline terrain, Sao Paulo State, Brazil. *Journal of Hydrology*, 357, 153-173.
- [22] Chung, C.J., and Fabbri, A.G., 2003. Validation of spatial prediction models for landslide hazard mapping. *Natural Hazards*, 30: 451-472.
- [23] Begueria, S. (2006). Validation and evaluation of predictive models in hazard assessment and risk management. *Natural Hazards*, 37(3), 315-329.
- [24] Tehrany, M.S., Pradhan, B., and Jebur, M.N. (2013). Spatial prediction of flood susceptible areas using rule based decision tree (DT) and a novel ensemble bivariate and multivariate statistical models in GIS. *Journal of Hydrology*, 504, 69-79.